24th INTERNATIONAL CONGRESS ON SOUND AND VIBRATION
23–27 July 2017, London

USING MEASURED BLOCKED FORCES TO PROVIDE REALISTIC EXCITATION OF VIRTUAL ACOUSTIC PROTOTYPES

Andy Moorhouse, Andy Elliott, Joshua W R Meggitt

University of Salford, Acoustics Research Centre, Salford, Greater Manchester, M5 4WT, UK
email: a.t.moorhouse@salford.ac.uk

The context of the paper is the need for prediction and simulation of vibro-acoustic response of assembled structures. Virtual Acoustic Prototypes (VAP) allow the responses to be auralised in addition to simple prediction. One of the main areas of difficulty when constructing a VAP is to know the excitation forces. The blocked force method allows vibration sources to be characterised independently using conventional measurements similar to those used in Transfer Path Analysis (TPA). The blocked forces are theoretically an invariant property of the source and hence remain valid when for example the same vibration source is attached to different receiver structures. Several previous studies have shown how the blocked forces can be used to provide accurate and realistic excitation for Virtual Acoustic Prototypes assembled using measured properties for the subsystems. The question is considered how to apply blocked forces to a new receiver which might be represented, for example, by a model.

Keywords: Blocked force, source characterisation, transfer path analysis, vibro-acoustic simulation

1. Introduction

The context of the paper is the need across many industries for prediction and simulation of vibro-acoustic response of assembled structures. Throughout the vast literature on vibro-acoustic simulation and modelling, surprisingly little attention is given to excitation of numerical models in a realistic way; typically models produce vibro-acoustic responses scaled to unit force excitation as output. The lack of data to describe excitation by active components is therefore arguably one of the biggest limitations of numerical models in vibro-acoustics at today's state of the art. In this paper we consider the characterisation of structure-borne sound sources based on experimental data and the use of this data to allow prediction of vibro-acoustic response in an assembly. In particular we focus on the use of blocked force data obtained using the in situ measurement method [1, 2]. The blocked forces concept is considered in the following section followed by some comments on their measurement and common sources of error. The use of this data in vibro-acoustic simulation is then discussed through two examples.

2. Source characterisation using blocked forces

Consider a source substructure installed on a receiver structure (see Fig. 1). The source substructure is excited by internal forces when operational, causing an operational response in the passive receiver structure B. The effect of the source on the receiver can be represented simply in terms of the contact forces at the interface, as in Fig. 1b which give an identical response field. This free body diagram approach is so well known that it hardly needs any explanation. Less well known is the second equivalent system, shown in Fig. 1c, in which the passive assembly of source and receiver is excited at the interface by a different set of forces. It turns out that the forces required to provide an identical response field in the receiver are none other than the blocked forces of the source, i.e. the forces which the operational source would exert on a perfectly rigid receiver [1, 2]. Depending on the sign convention used, these forces may also be considered the negative blocked forces, but this difference is trivial. Thus, the response field in the receiver can be represented in two equivalent forms:

$$\mathbf{y} = \mathbf{H}^{B}\,\mathbf{f} = \mathbf{H}^{AB}\hat{\mathbf{f}}. \tag{1}$$

where $\mathbf{y}$ is the vector of the response field in the receiver, $\mathbf{H}^{B}$, $\mathbf{H}^{AB}$ are the receiver FRF and coupled FRF of the assembly and $\mathbf{f}, \hat{\mathbf{f}}$ are the force and blocked force vector respectively. The first form on the rhs of Eq. 1 corresponds to Fig 1b and the second form to Fig 1c. The major potential advantage of the second formulation is that, whereas the contact forces applied by a source are a function of the receiver and therefore vary from one installation to the next, the blocked forces on the other hand are theoretically an invariant property of the source and can therefore be transferred from one installation to another, for example from a test bench to a real installation. The implications will be explored later in the paper. It is this transferable property which is the key to source characterisation using the blocked forces concept and the subsequent excitation of virtual acoustic prototypes and models. It will be seen that blocked forces provide the active part of a source characterisation; a full source characterisation also requires the passive properties of the source, particularly the FRFs, to be known in addition.

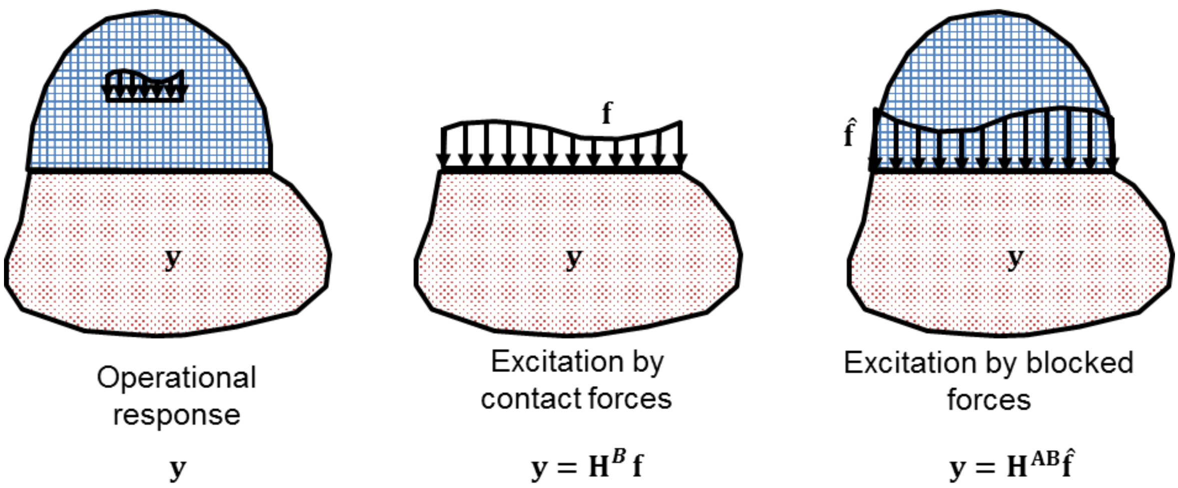

Figure 1: (a) Operating source on receiver (b) free body diagram of receiver where $\mathbf{H_B}$ are the FRFs of the receiver substructure (c) equivalent blocked force excitation where $\mathbf{H}^{\boldsymbol{AB}}$ are the FRFs of the assembly.

3. Measurement of blocked forces

The second form of equation 1 provides the theoretical basis for obtaining the blocked forces by inverse methods. The blocked force vector is given by solving the second form of Eq (1):

$$\mathbf{H}^{\boldsymbol{AB}^{+}}\mathbf{y} = \hat{\mathbf{f}}. \tag{2}$$

where $\mathbf{H}^{\boldsymbol{AB}^{+}}$ is the inverse, or pseudo inverse of $\mathbf{H}^{\boldsymbol{AB}}$.

As will be discussed later, it is important to include all the forces which excite the receiver substructure and therefore an important step prior to any measurements is to define the interface between the source and receiver and to identify all active degrees of freedom. Having defined the interface, a two-stage measurement method is employed:

(a) An operational stage in which the responses $\mathbf{y}$ are measured in the receiver with the source in normal operation. Measurements are normally made with accelerometers at, or close to the source-receiver interface;

(b) A passive measurement stage in which the FRFs $\mathbf{H}^{AB}$ are measured, typically using a hammer or shaker.

The most common types of error are due to incompleteness or inconsistency in the measured data set. Incompleteness refers to missing degrees of freedom, which are discussed in the following section. Regarding consistency, measurements to obtain $\mathbf{H}^{AB}$ and $\mathbf{y}$ are made at different times and under different conditions but everything possible should be done to ensure that the two data sets are as consistent as possible. For example, if accelerometers are removed and replaced between tests and are not replaced in exactly the same location there will be inconsistency between $\mathbf{H}^{AB}$ and $\mathbf{y}$ which can cause large errors during inversion. Therefore, it is desirable to leave accelerometers attached for both tests. Another cause of inconsistency is that measurement points on the interface do not coincide exactly with the location of the actual interface forces.

3.1 Errors due to neglected degrees of freedom

Considering the completeness of the data set, Eq (1) is exact for linear, time-invariant systems, provided that all excitation forces at the source-receiver interface are included. In practice, a common source of error is to neglect some interface degrees of freedom, because they are either unknown or too difficult to measure, for example rotations and/ or in-plane forces for which measurement of FRFs is notoriously difficult. Therefore, it is instructive to consider the errors that are caused by neglected dofs at the interface.

If we partition the interface dofs into those which are known, given subscript *k*, and those which are unknown or omitted for other reasons, given subscript *u*, we obtain the following instead of Eq. (1):

$$\mathbf{y} = [\mathbf{H}_{bk} \quad \mathbf{H}_{bu}] \begin{bmatrix} \hat{\mathbf{f}}_k \\ \hat{\mathbf{f}}_u \end{bmatrix}. \tag{3}$$

where the subscript b refers to selected points on the receiver structure which may be anywhere, including at the interface. To obtain the blocked forces by inversion, Eq. (3) is pre-multiplied by the inverse (or pseudo inverse) of the FRF matrix relating to the known dofs $\mathbf{H}_{bk}^{+}$ giving:

$$\hat{\mathbf{f}}_{meas} = \mathbf{H}_{bk}^{+}\,\mathbf{y} = \hat{\mathbf{f}}_k + \mathbf{H}_{bk}^{+}\,\mathbf{H}_{bu}\hat{\mathbf{f}}_u \tag{4}$$

where $\hat{\mathbf{f}}_{meas}$ are the blocked forces obtained from consideration of only the known interface dofs. The first term on the right hand side represents the true blocked forces at these dofs and the second term represents an error. Thus, by neglecting unknown degrees of freedom not only is the description of the source is incomplete, since it does not include unknown dofs, but the 'known' forces which *are* included contain errors given by the second term in Eq (4). Furthermore, the approximate blocked forces obtained are no longer strictly an independent property of the source since the matrix $[\mathbf{H}_{bk}^{+}\,\mathbf{H}_{bu}]$ in Eq (4) is constructed from FRFs of the assembly. The effect will be minimised when the transfer FRF $\mathbf{H}_{bu}$ is small. However, in general the transferability of the blocked forces is compromised when dofs are omitted,

3.2 Design of test receiver

Tests may be conducted in situ, i.e. with the source installed in a real installation, or on a specially designed test bench. The factors to consider in the choice of test arrangement are:

a) representativeness of the receiver in terms of its effect on source mechanisms;
b) design of the test receiver for ease of access to interface dofs.

In the case of an in situ test, the test environment is representative by definition. In the case of a test bench, the test receiver is different to that of the intended installation and it should be considered whether there could be any influence on the source mechanisms. There is little information about this issue, but a reasonable approach seems to be to use a test bench that is dynamically similar to the receiver substructure of the intended installation. Further work is needed to define the precise meaning of 'dynamically similar' although Eq. (4) provides some insight. In practical terms, it seems sensible to avoid rigid mounting to a test bench if the intended installation is on resilient mounts and *vice versa*.

Regarding access, it is easier to obtain good FRF data when there is good access to measurement points and given that poor measurements is a main reason for poor results it makes sense to design a test bench so as to make it easy to access the required measurement points.

4. Blocked force transfer path analysis

Blocked force transfer path analysis (also known as in situ TPA or iTPA) includes, in addition to the inverse step described above, a forward calculation to predict the response at 'new' dofs on the assembly [3, 4]. Eq. (1) is extended so as to include the response at prediction points, given the subscript p

$$\begin{bmatrix}\mathbf{y}_b\\ \mathbf{y}_p\end{bmatrix} = \begin{bmatrix}\mathbf{H}_{bc}\\ \mathbf{H}_{pc}\end{bmatrix}\widehat{\mathbf{f}_c}. \tag{5}$$

where $c = k \cup u$ refers to the complete set of interface dofs and b are measurement points on the receiver used in the inverse calculation. Typically, b are close to the interface and may fully or partially coincide with the interface dofs c. For example, for a road noise TPA, the b points are typically located on the suspension and the prediction points p in the vehicle cabin. The first row of Eq (5) is solved as an inverse problem to obtain the blocked forces $\widehat{\mathbf{f}_c}$ which are then used for a forward prediction using the second row. The diagnostic value of TPA is that the contributions of the components of $\widehat{\mathbf{f}_c}$ to the predicted output $\mathbf{y}_p$ can be quantified.

In the case where an incomplete set of interface dofs has been used then, picking up the analysis from section 3.1 above, the interface dofs can again be partitioned into known (k) and unknown (u) sets. The true output at the prediction position is then:

$$\mathbf{y}_p = \mathbf{H}_{pc}\widehat{\mathbf{f}_c} = [\mathbf{H}_{pk} \quad \mathbf{H}_{pu}]\begin{bmatrix}\hat{\mathbf{f}}_k\\ \hat{\mathbf{f}}_u\end{bmatrix} = \mathbf{H}_{pk}\hat{\mathbf{f}}_k + \mathbf{H}_{pu}\hat{\mathbf{f}}_u. \tag{6}$$

However, instead of the true blocked forces we have from Eq. (4):

$$\widehat{\mathbf{f}_c} = \begin{Bmatrix}\widehat{\mathbf{f}_k}\\ \widehat{\mathbf{f}_u}\end{Bmatrix} \to \begin{Bmatrix}\hat{\mathbf{f}}_{meas}\\ \mathbf{0}\end{Bmatrix} = \begin{Bmatrix}\hat{\mathbf{f}}_k + \mathbf{H}_{bk}^{+}\,\mathbf{H}_{bu}\hat{\mathbf{f}}_u\\ \mathbf{0}\end{Bmatrix}. \tag{7}$$

which, by substituting Eq.(7) into Eq. (6) gives a predicted output as follows:

$$\mathbf{y}_{p,meas} = \mathbf{H}_{pk}\hat{\mathbf{f}}_{meas} = \mathbf{H}_{pk}\hat{\mathbf{f}}_k + \mathbf{H}_{pk}\mathbf{H}_{bk}^{+}\,\mathbf{H}_{bu}\hat{\mathbf{f}}_u. \tag{8}$$

Comparing Eqs. (6) and (8) we see that the predicted output differs from the true output in the second term: $\mathbf{H}_{pu} \to \mathbf{H}_{pk}\mathbf{H}_{bk}^{+}\,\mathbf{H}_{bu}$. These terms are equal when prediction points coincide with the b point (since $\hat{\mathbf{f}}_{meas}$ was calculated so as to enforce this equality). However, Eq. (8) shows that the unknown blocked forces are accounted for to some extent despite not having been identified explicitly.

5. Blocked forces in vibro-acoustic prediction

We now consider the more general case where we wish to predict responses in a different receiver. TPA allows for prediction of response in an already existing receiver for the purposes of diagnostics. However, the ultimate goal of source characterisation is for prediction of responses in combinations of the source with new receivers, including not-yet-existing structures represented by models.

The prediction is described by the lower row of Eq (5), however, the FRF is now for a new combination of the source with a different receiver.

$$\mathbf{y}_{p}^{AC} = \mathbf{H}_{pc}^{AC}\hat{\mathbf{f}_{c}}. \tag{10}$$

where the superscript AC indicates a combination of source substructure A with new receiver C. The FRFs for the assembly may be expressed in terms of the substructure FRFs (suffices A, C) as:

$$\mathbf{H}_{pc}^{AC} = \mathbf{H}_{pc}^{C}\left[\mathbf{H}_{cc}^{C} + \mathbf{H}_{cc}^{A}\right]^{-1}\mathbf{H}_{cc}^{A} \tag{11}$$

This will be recognised as a substructuring step which is known to be difficult to implement in practise despite its simplicity from a theoretical point of view. Various forms of Eq (9) have been proposed to try to reduce errors in the calculation of assembly properties from those of its substructures [5]. It is suggested here that when one of the substructures (typically C) is modelled, then it may be easier to obtain consistency by also modelling the source structure (A) rather than trying to combine measured and modelled data which is bound to be inconsistent to some extent. However, the aim here is not to further investigate the substructuring step itself but rather to consider the effects of injecting blocked forces into a substructured assembly.

Repeating the analysis that led to Eq (8), but recognising that the inverse step occurs in assembly AB whereas the forward step occurs in assembly AC we obtain.

$$\mathbf{y}_{p}^{AC} = \mathbf{H}_{pk}^{AC}\hat{\mathbf{f}}_{k} + \mathbf{H}_{pk}^{AC}\mathbf{H}_{bk}^{AB^{+}}\ \mathbf{H}_{bu}^{AB}\hat{\mathbf{f}}_{u}. \tag{12}$$

The first term, consisting of the known forces, is seen to be free from any influence of the test bench (substructure B) but this is not the case for the second term. Thus, we see again how the independence of the blocked forces is compromised by neglected dofs.

6. Example results

In this section two examples are presented where blocked force data has been used to excite a new virtual assembly. In the first case, blocked forces for a building-mounted wind turbine were used to excite an empirical model of a building. In the second case, a small pump, used in aerospace applications was virtually mounted on a plate via isolators.

6.1 Small wind turbine example

The first example is the prediction of sound pressure levels inside a building to which a building mounted wind turbine is attached. The steps in the analysis are summarised in Fig. 2 and are explained in more detail in [6, 7]. The blocked forces were obtained for two different wind turbines in a series of field tests over a range of rotational speeds. The mounting mast and brackets were separately characterised in the laboratory using a transmissibility technique and the vibro-acoustic FRFs were obtained empirically from a survey of tests on cavity and solid brick buildings.

Finally, the sound pressure level in the building was predicted and compared with some snapshot measurements made in windy conditions inside a building. The sound pressure was predicted from

$$\boldsymbol{p} = \mathbf{H}_{pc}^{C}\mathbf{T}\hat{\mathbf{f}} \tag{11}$$

Where H_{pc}^{C} are FRFs of the building and $\mathbf{T}$ is the transmissibility of the mast. Note that in this case, because the building is of a massive construction it was possibly to make the simplifying assumption that the coupled FRFs of the assembly were equal to those of the receiver alone, i.e.:

$$\mathbf{H}_{pc}^{AC} = \mathbf{H}_{pc}^{C}\left[\mathbf{H}_{cc}^{C} + \mathbf{H}_{cc}^{A}\right]^{-1}\mathbf{H}_{cc}^{A} \approx \mathbf{H}_{pc}^{C} \tag{11}$$

Some major assumptions were necessary to allow an answer to be obtained, notably, first, that the blocked forces were repeatable for a given shaft speed (in fact there was considerable variation due to varying turbulence, electronic control inherent in the turbine and a range of other factors. Secondly, since external access was not available for the installation building, the FRFs had to be estimated from measurements obtained across a range of similar buildings. Considering the extent of these (and other) assumptions the agreement with direct measurement was considered acceptable. Note that it was at least possible to obtain some sensible answer and it is difficult to imagine how this could have been done at all except with the in situ blocked force method.

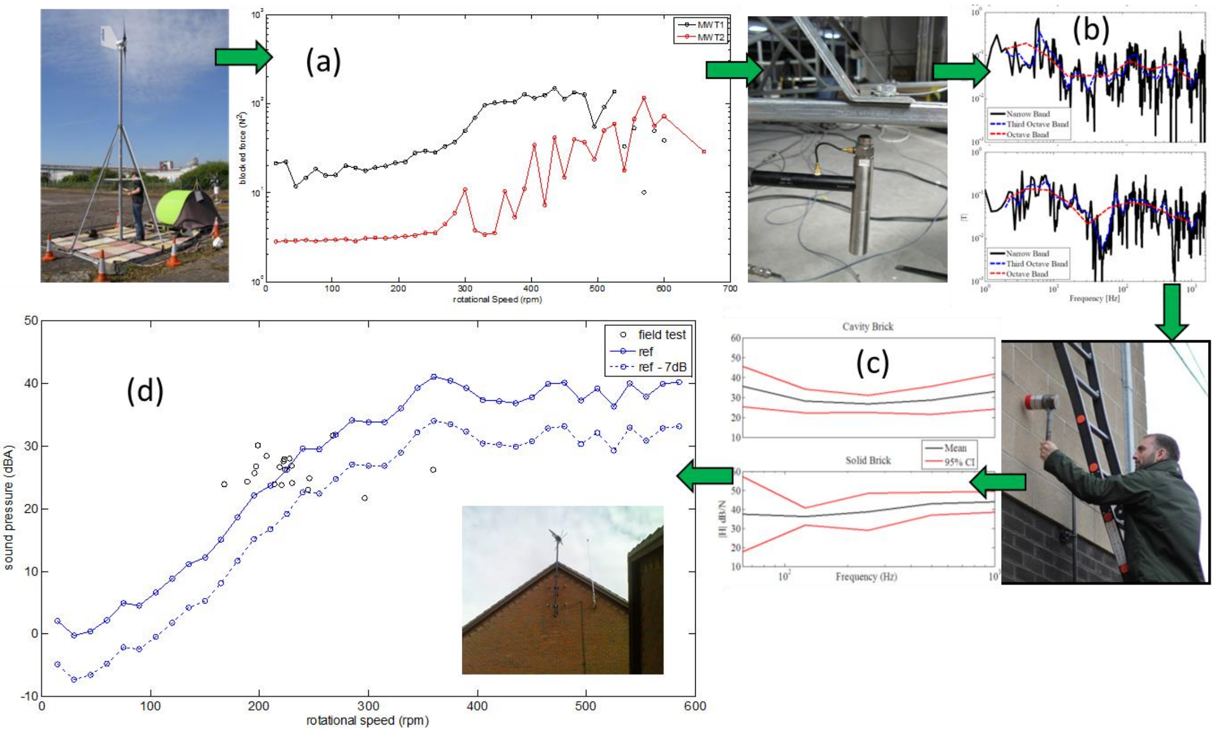

Figure 2: Procedure used to obtain predictions of the sound pressure level inside buildings due to wind turbines mounted on the external walls: (a) measurement of blocked force; (b) experimental characterisation of mounting: (c) experimental characterisation of a range of buildings; (d) prediction of sound pressure level in a new building, compared with direct measurement (dots -7dB is the correction for rooms not immediately next to the wind turbine).

6.2 Pump on isolators

In the second example the velocity response from a four-footed, resiliently-mounted electric pump used in aerospace applications is predicted (see Fig. 3).

Blocked forces are first obtained from the in situ method with the pump attached to a small perspex plate serving as a test bench. The pump is then transferred to a large, thicker perspex receiver plate which represents the new installation. As shown in Fig. 2, the velocity response in the plate is predicted from the blocked forces combined with:

a) FRFs for the new assembly which were measured directly (blue curve)
b) FRFs for the new assembly obtained by mathematically combining separate FRFs for the plate, isolators and pump (red curve). The isolator dynamic stiffness was obtained from an in situ method described in [8].

Good results were obtained, and an auralisation of these results (to be played at the conference) indicates that it is difficult to tell the difference between directly recorded sounds and those synthesised from the blocked force and substructuring approach. Thus, the prediction is sufficiently accurate for auralisation purposes. This study is a relatively simple case in that the resilient couplings allow degrees of freedom other than the vertical to be neglected in the substructuring step. Nevertheless, it is a realistic case and demonstrates the potential of this approach.

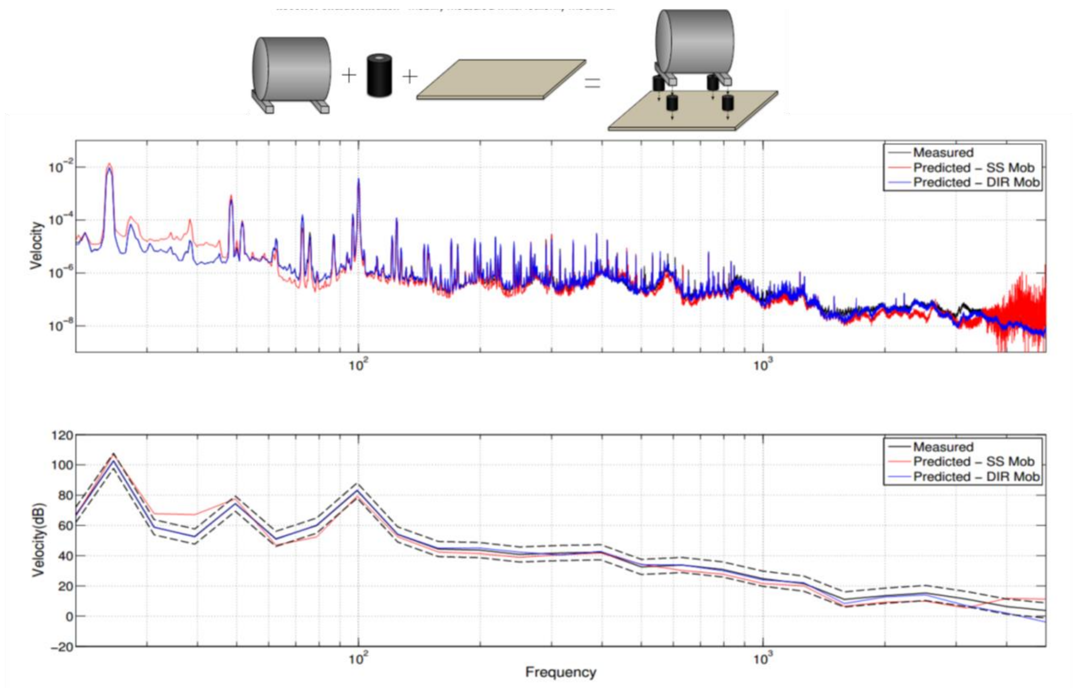

Figure 3: Measured velocity in a plate excited by a pump compared with that calculated from blocked forces obtained from a separate test rig: blue curve- blocked forces combined with measured assembly FRFs; red curve – blocked force combined with assembly FRFs calculated from separate substructure FRFs.

7. Concluding remarks

In the field of vibro-acoustic simulation and virtual acoustic prototypes it has been argued that the excitation of the models remains one of the main unsolved areas. The blocked force method has been presented which potentially provides a general and practical approach for realistic excitation of such models based on the blocked forces measured on another installation or test bench. Two steps are required, each of which contains an inherent practical challenge:

a) the inverse step to obtain the blocked forces requires particular care to avoid large errors on inversion;
b) secondly, for the forward prediction a substructuring step is required which, again is known to be delicate and requires particular care.

Consistency and completeness of the measured data seem to provide the keys to this theoretically simple but practically very challenging problem. Regarding incompleteness, it has been shown that the independence of the blocked forces is compromised if degrees of freedom are omitted at the interface. To avoid inconsistency between models and test data, it has been suggested that both source and receiver substructures should be modelled prior to the injection of (measured) blocked forces so as to avoid the need to combine measured and modelled FRF data.

Experimental examples have been presenting which show that good results can be obtained with sufficient care. Additional examples are given in e.g. [9]. Further results indicating the excitation of models will be presented at the conference.

Acknowledgements

This work was partially supported by the Engineering and Physical Sciences Research Council, EPSRC [grant ref. EP/P005489/1]. The support of the Department for Environment, Food and rural Affairs (defra) for the wind turbine case study. Both funders are gratefully acknowledged.

REFERENCES

1 Bobrovnitskii, Y.I., 2001. A theorem on the representation of the field of forced vibrations of a composite elastic system. *Acoustical Physics*, *47*(5), pp.507-510.

2 Moorhouse, A.T., Elliott, A.S. and Evans, T.A., 2009. In situ measurement of the blocked force of structure-borne sound sources. *Journal of Sound and Vibration*, *325*(4), pp.679-685.

3 van der Seijs, M.V., de Klerk, D. and Rixen, D.J., 2016. General framework for transfer path analysis: History, theory and classification of techniques.*Mechanical Systems and Signal Processing*, *68*, pp.217-244.

4 Elliott, A.S., Moorhouse, A.T., Huntley, T. and Tate, S., 2013. In-situ source path contribution analysis of structure borne road noise. *Journal of Sound and Vibration*, *332*(24), pp.6276-6295.

5 Klerk, D.D., Rixen, D.J. and Voormeeren, S.N., 2008. General framework for dynamic substructuring: history, review and classification of techniques. *AIAA journal*, *46*(5), pp.1169-1181.

6 Elliott, A.S. and Moorhouse, A.T., 2010. In-situ characterisation of structure borne noise from a building mounted wind turbine. *Proc. ISMA2010.*

7 Moorhouse, A., Elliott, A., Eastwick, G., Evans, T., Ryan, A., von Hunerbein, S., Le Bescond, V. and Waddington, D., 2011. Structure-borne sound and vibration from building-mounted wind turbines. *Environmental Research Letters*, *6*(3), p.035102.

8 Meggitt, J.W.R., Elliott, A.S., Moorhouse, A.T. and Lai, H.K., 2016. In situ determination of dynamic stiffness for resilient elements. *Proceedings of the Institution of Mechanical Engineers, Part C: Journal of Mechanical Engineering Science*, *230*(6), pp.986-993.

9 Lennström, D., Olsson, M., Wullens, F. and Nykänen, A., 2016. Validation of the blocked force method for various boundary conditions for automotive source characterization. *Applied Acoustics*, *102*, pp.108-119.